Available online at www.sciencedirect.com

ScienceDirect

Ceramics International 40 (2014) 447–452

CERAMICS INTERNATIONAL

www.elsevier.com/locate/ceramint

Nanocrystalline Ce doped $CoFe_2O_4$ as an acetone gas sensor

M.S. Khandekar[a], N.L. Tarwal[b,c], I.S. Mulla[d], S.S. Suryavanshi[a,*]

[a]*Ferrite Materials Laboratory, Department of Physics, Solapur University, Solapur 413255, India*
[b]*Research Institute for Solar and Sustainable Energies (RISE), Gwangju Institute of Science and Technology (GIST), Gwangju 500712, Republic of Korea*
[c]*School of Information and Communications, Gwangju Institute of Science and Technology (GIST), Gwangju 500712, Republic of Korea*
[d]*Physical Chemistry Division, National Chemical Laboratory, Pune 411008, India*

Received 25 May 2013; received in revised form 6 June 2013; accepted 10 June 2013
Available online 15 June 2013

Abstract

Nanocrystalline $CoFe_{2-x}Ce_xO_4$ ferrites ($x=0$, 0.04, 0.08) were synthesized by using the inexpensive, simple and eco-friendly molten-salt (M-S) method. Effects of Ce doping on the structural, morphological and gas sensing properties of the $CoFe_2O_4$ ferrite were investigated. X-ray diffraction (XRD) analysis revealed the formation of spinel $CoFe_2O_4$. Transmission electron microscopy (TEM) investigations showed that the synthesized ferrite is made up of very fine spherical nanoparticles. Furthermore, the gas response of nanocrystalline ferrite materials was investigated in the temperature range of 200–450 °C toward the reducing gases like liquefied petroleum gas (LPG), acetone, ethanol and ammonia. The sensor response was found to be sensitive and selective toward acetone as compared to other reducing gases. It is observed that the addition of Ce (4 wt%) strongly influenced the response and the operating temperature of the sensor material and thus can serve as acetone-sensing sensors.

Keywords: D. Ferrite; $CoFe_2O_4$; Gas sensor; Molten-salt method; TEM

1. Introduction

The demand of chemical sensor has been increased due to its ability to regulate the emissions and detection of hazardous pollutants. Among the various chemical sensors, metal oxide semiconductor sensors are the most promising as they provide many advantages such as low cost, small dimensions, low power consumption, on-line operation. They are highly compatible with microelectronic processing and hence they have been investigated widely for long time [1]. Recently, the gas sensing applications of nanocrystalline materials have received considerable interest [2,3]. The ferrites have demonstrated to be good materials for semiconductor gas sensors [4–6]. A semiconductor gas sensor presents the property of changing the conductivity of the sensing material when this is exposed to different gas atmospheres.

The gas-sensing is a surface controlled process, which is based on the reaction between adsorbed oxygen and gas molecules to be detected. The gas response of the sensor usually depends on the operating temperature, gas species and sensor material [7]. Over the all spinel-type metal oxide semiconductor sensors, the oxides with a general formula of AB_2O_4 are important for gas sensor applications, and have been investigated for the detection of both oxidizing and reducing gases. The spinel ferrites such as $ZnFe_2O_4$, $MnFe_2O_4$, $NiFe_2O_4$ and $CoFe_2O_4$ have shown good sensitivity for variety of gases, because of their stability in thermal and chemical atmospheres, fast response and recovery time, low cost and simple electronic structure [8–11]. Particularly, $CoFe_2O_4$ has attracted considerable attention in recent years due to its unique physical properties such as high Curie temperature, large magneto-crystalline anisotropy, high corecivity, moderate saturation magnetization, large magneto-strictive coefficient, excellent chemical stability and mechanical hardness [12]. It has inverse spinel structure with Co^{2+} ions in octahedral sites and Fe^{3+} ions equally distributed between tetrahedral and

*Corresponding author. Tel.: +91 217 2744771; fax: +91 217 2744770.
E-mail address: sssuryavanshi@rediffmail.com (S.S. Suryavanshi).

0272-8842/$ - see front matter © 2013 Elsevier Ltd and Techna Group S.r.l. All rights reserved.
http://dx.doi.org/10.1016/j.ceramint.2013.06.021

octahedral sites and has been demonstrated in the literature based on the preference energies for divalent and trivalent ions in the spinel structure [13].

Large variety of synthesis techniques used to obtain nano-sized spinel ferrite powders, including the standard ceramic technique, molten-salt method, co-precipitation, microemulsion, micelle and hydrothermal methods and sol–gel process [14–21]. Among the various methods, the molten-salt method is a convenient, eco-friendly and inexpensive method for the preparation of ferrites at low processing temperature in short duration [21].

Doping is an important and effective route to fine tune the desired properties of semiconductors [22–26]. The dopant could enhance gas-sensing properties of metal-oxide semiconductor by changing energy-band structure, mending the morphology and surface-to-volume ratio, and creating more active center at the grain boundaries [27]. Another route for the enhancement of the gas sensing properties is sensitization with the noble metals, where it acts as a catalyst, which is not only promote gas response but also improve the response time [28,29].

In our previous report, we have studied the gas sensing performances of pure $CuFe_2O_4$ and Ce doped $CuFe_2O_4$ materials synthesized by using a simple M-S method [30]. In the present work, we report here the synthesis of pure and Ce doped $CoFe_2O_4$ material using a simple M-S method and its application as a gas sensor. These ferrites have been tested towards four reducing gases such as LPG, acetone, ethanol and NH_3 and results are presented here.

2. Experimental

The raw materials used for ferrite synthesis were analytical reagent grade $CoSO_4 \cdot 7H_2O$, $Fe(NO_3)_3 \cdot 9H_2O$, NaOH, and NaCl. These chemicals were dry mixed in the molar ratio (1:2:8:10) and ground together with an appropriate quantity of $Ce(NO_3)_2.6H_2O$ (0, 4 and 8 wt%) in agate mortar for 90 min. During mixing, the reaction started voluntarily, accompanied by the release of heat. The mixture initially turned mushy and underwent gradual changes from colorless to light red in a few minutes and finally turned black. The mixture was then heated at 400 °C for 2 h and subsequently cooled to room temperature. Finally the samples were thoroughly washed with distilled water, dried under IR lamp. The resulting dry decomposed powder was mixed with polyvinyl acetate as a binder to prepare pellets. The disks of about 2 mm thickness and 15 mm in diameter were formed using the manual hydraulic press machine at pressure of 1.5 tonn/cm^2 and sintered at 700 °C for 2 h in order to increase the mechanical strength. These sintered undoped (0 wt%) and cerium doped (4 wt% and 8 wt%) $CoFe_2O_4$ samples are denoted as Ce0, Ce4 and Ce8, respectively.

The structural studies of the sintered samples were characterized by using a Philips PW-3710 powder X-ray diffractometer with CuK_α radiation with wavelength, $\lambda = 0.154056$ nm. The particle sizes of the sintered ferrite samples were observed by using transmission electron microscopy (TEM) with PHILIPS CM-200 model. The gas response properties of the sintered pellets were studied using the commercial setup earlier reported [31]. The electrical resistance of the sensor was measured in the presence of air and with relevant test gases. The gas response (S) was defined as the ratio of the electrical resistance in sample gases (R_g) to that in air (R_a).

3. Results and discussion

3.1. Structural studies

Using the XRD with CuK_α radiation, the phase identification of the ferrite samples was carried out. Fig. 1(a)–(c) shows the recorded XRD patterns over 20–80° for Ce0, Ce4 and Ce8 ferrite samples, respectively. Fig. 1(a) shows diffraction peaks at $2\theta = 30.1°$, 35.4°, 43.1°, 53.6°, 57.0° and 62.6°, which corresponds to the crystal indexes of (220), (311), (400), (422), (511), and (440), respectively. All the diffraction peaks can be indexed to the cubic crystal structure of cobalt ferrite (JCPDS card no. 22-1086). Similar XRD pattern is also obtained after Ce 4% doping (Fig.1(b)). However after Ce (8%) doping, obtained XRD pattern (Fig.1(c)) shows the presence of mixed phases with peaks corresponding to spinel type structure of $CoFe_2O_4$ and less intense peaks corresponding to CeO_2 (JCPDS card no. 81-0792) phase. It is observed that the peak intensity of (311) peak increases with Ce doping content. The lattice parameter (a) for each composition was calculated (given in the Table 1) using the formula ($a = [d^2(h^2+K^2+l^2)]^{1/2}$), where, ($hkl$) are miller indices of the crystal planes which are in close agreement with those given in the JCPDS files No. (22-1086) of $CoFe_2O_4$. The variation of lattice parameters is due to their difference in the ionic radii (Ce = 1.034 Å, Fe = 0.645 Å). All diffraction peaks are the characteristics of the constituent's phases. No peaks other than this material are observed. The average crystallite size (D) was calculated from line

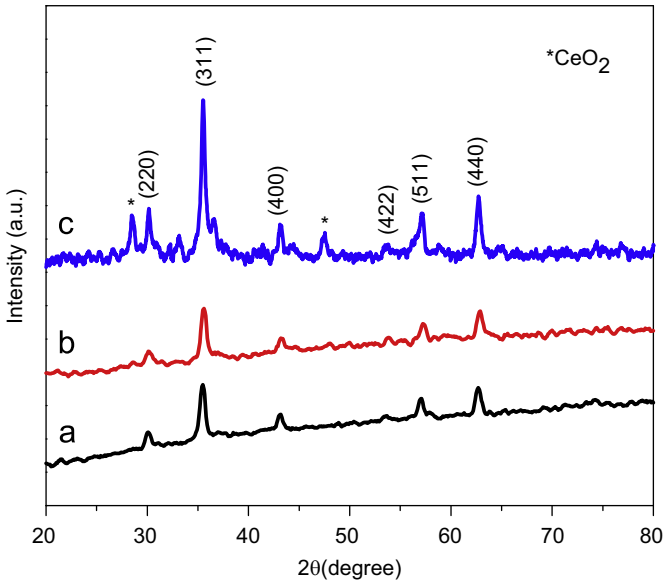

Fig. 1. X-ray diffraction patterns of the (a) Ce0, (b) Ce4 and (c) Ce8 ferrite samples.

Table 1
The calculated crystallite size, D (nm) and lattice parameter, a (Å) of the Ce0, Ce4 and Ce8 samples.

Sample code	Materials	Crystallite size, D (nm)	Lattice parameter, a (Å)
Ce0	$CoFe_2O_4$	28	8.385
Ce4	$CoCe_{0.04}Fe_{1.96}O_4$	13	8.372
Ce8	$CoCe_{0.08}Fe_{1.92}O_4$	25	8.417

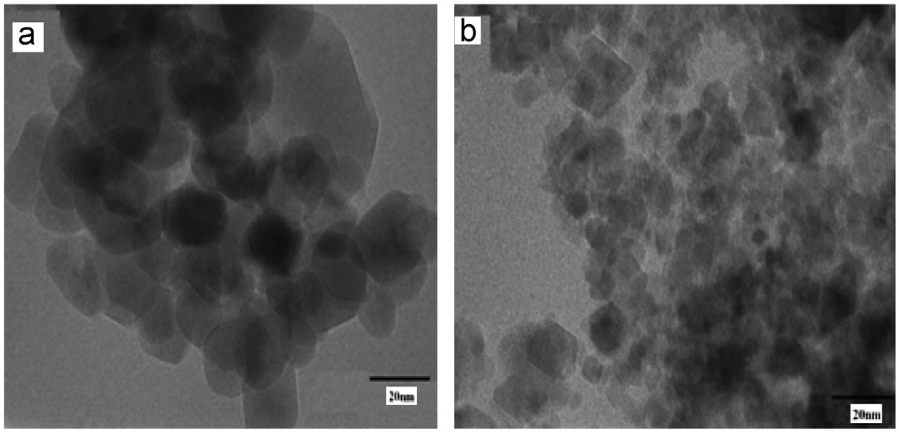

Fig. 2. TEM images of the (a) Ce0 and (b) Ce4 ferrite samples.

broadening of (311) reflection using Debye-Scherrer's formula:

$$D = \frac{0.9\lambda}{\beta Cos\theta} \quad (1)$$

Where, λ is the wavelength of X-ray used, β is the full width at half maximum (FWHM) of the most intense diffraction peak and θ is the Bragg's angle for the actual peak.

The average crystallite size of undoped and Ce doped $CoFe_2O_4$ samples are presented in Table 1. It is seen that the calculated crystallite size for Ce4 ferrite sample is less compared to other samples.

3.2. Morphological studies

The obtained TEM images for Ce0 and Ce4 ferrite samples are shown in Fig. 2(a) and (b), respectively. The TEM image of Ce0 sample [Fig. 2(a)] shows uniformly distributed spherical nanoparticles having diameter of 20 nm. After Ce incorporation the significant reduction in particle size ~10 nm is found from TEM of the Ce4 sample, as shown in Fig. 2(b). This significant reduction in the ferrite nanoparticles is due to Ce incorporation. The observed particle sizes from the TEM findings for these ferrite samples are well matched with the calculated average crystallite sizes from XRD. Rezlescu et al. [32] have shown 2 wt% Ce doped Ni–Zn ferrite material exhibits well developed grains and their grain size was found to decrease after Ce doping. Such a small and well-distributed ferrite nanoparticles are highly suitable for gas sensing application.

3.3. Gas sensing properties

The sensitivity toward reducing gases such as LPG, acetone, ethanol and ammonia was investigated at different operating temperatures in 2000 ppm of test gas at various operating temperatures in the range of 200–450 °C, to avoid the effect of the surface adsorbed water [33]. Niu et al. [34] reported the formula for p-type sensors for calculation of response towards reducing gases as $S = R_g/R_a$. In the present work, we observed undoped and Ce doped $CoFe_2O_4$ as p-type sensors so have calculated the sensitivity (S), using the relation:

$$S(\%) = \frac{R_g}{R_a} \times 100 \quad (2)$$

Where, R_a is the sensor resistance in the air and R_g is the sensor resistance in the presence of test gas at a given temperature.

In order to determine the optimum working temperature of the sensor, the response were examined as a function of temperature for 2000 ppm of various gas/vapor species. From Fig. 3(a, c and e), it is seen that the ferrite material possesses a maximum sensitivity to each gas corresponding to an optimum working temperature. It is also observed that the $CoFe_2O_4$ exhibit a characteristic p-type semiconducting behavior as there is increase in resistance of the sensor, when it is exposed to reducing gas. The Ce0 sensor exhibits maximum response of 146, 139, 130, and 112% toward acetone, ethanol, LPG and ammonia, respectively at the same operating temperature 350 °C, as shown in Fig. 3(a). The response time for the Ce0 sensor towards acetone is found to be 50 s and recovery time is of 106 s. Fig. 3(b) shows the variation of response with

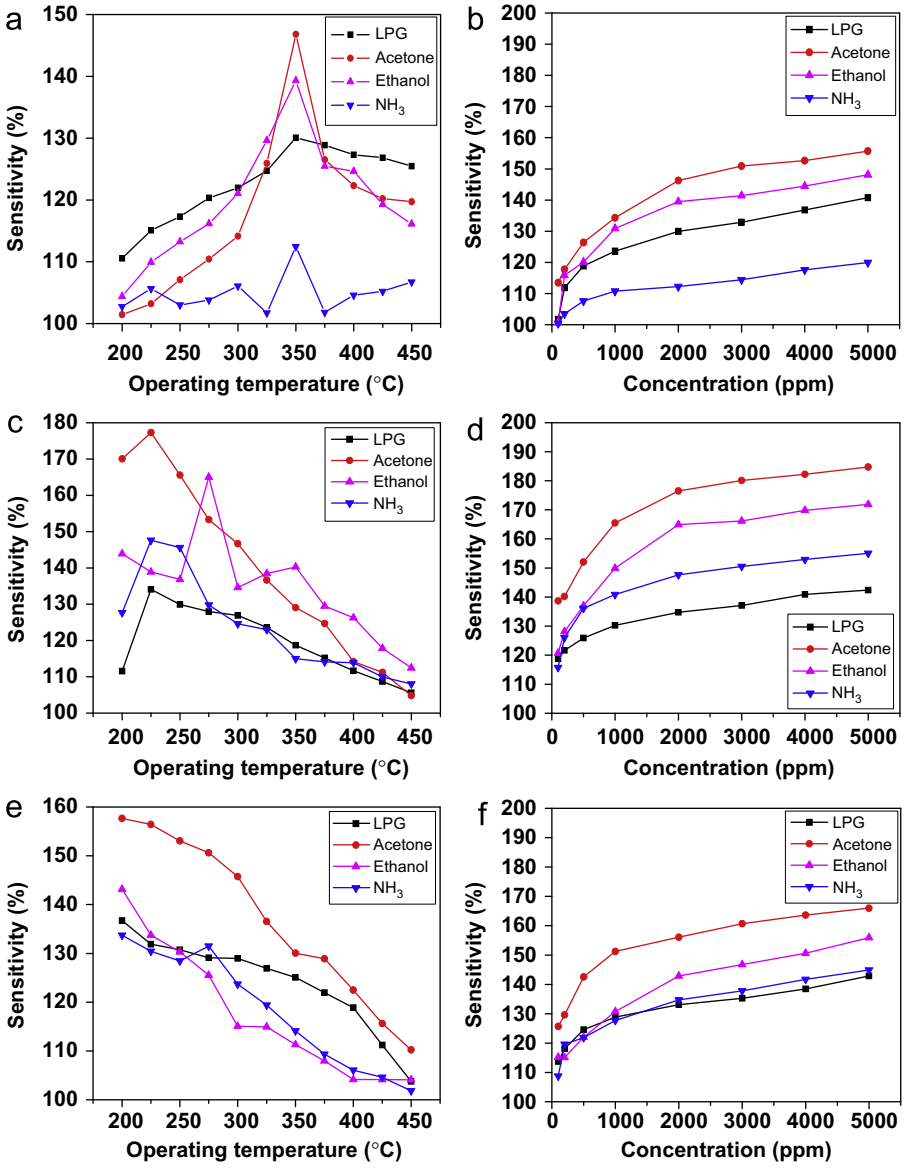

Fig. 3. Gas sensing response of (a) Ce0, (c) Ce4 and (e) Ce8 ferrite sensors toward the LPG, acetone, ethanol and ammonia gases at various operating temperatures. The variation of gas sensitivity with concentration of test gas for (b) Ce0, (d) Ce4 and (f) Ce8 ferrite sensor, respectively.

concentration of test gas for Ce0 sensor. It is found that the response increases with increase in concentration from 100 ppm up to 2000 ppm, above 2000 ppm it remains almost constant.

The variation of gas response as a function of operating temperature for Ce4 sensor is shown in Fig. 3(c). For Ce4 sample it is observed that the response was found to increases up to 177% for acetone, 134% for LPG, 147% for ammonia at the same operating temperature 225 °C while for ethanol it is 165% at 275 °C in comparison with Ce0 sensor. It is noted that Ce4 sensor exhibits higher response for all test gases as compared to Ce0 sensor. This increment is due to the smaller and well-distributed ferrite nanoparticles as observed from TEM investigations. The response time of the Ce4 sensor is found to be 45 s and recovery time 70 s which is reduced in comparison to Ce0 sensor. The variation of response with test gas concentration for Ce4 sensor is shown in Fig. 3(d). The response is found to increase with test gas concentration increases from 100 ppm up to 2000 ppm, and above 2000 ppm it remains constant up to 5000 ppm.

Fig. 3(e) depicts the variation of gas response with operating temperature for Ce8 sensor. The maximum response of 157% for acetone, 143% for ethanol, 137% for LPG and 134% for ammonia was observed at the same operating temperature 200 °C. The response time and recovery time for Ce8 sensor is found to be 38 s and 61 s, respectively. Fig. 3(f) exhibits the variation of response with test gas concentration for Ce8 sensor. The response increases with test gas concentration increases from 100 ppm up to 2000 ppm, above 2000 ppm it remains almost constant.

The observed acetone gas response values at optimum operating temperature for pure $CoFe_2O_4$ (Ce0) and Ce doped $CoFe_2O_4$ ferrite samples with different Ce doping concentrations (Ce4 and Ce8) are tabulated in Table 2. Also the response and recovery time for these sensors are given therein.

Table 2
The observed acetone gas response at optimum operating temperature for pure $CoFe_2O_4$ and Ce doped $CoFe_2O_4$samples with different Ce doping concentrations.

Sample code	Optimum operating Temperature, T_{OP} (°C)	Acetone gas response (%)	Response time (s)	Recovery time (s)
Ce0	350	146	50	106
Ce4	225	177	45	70
Ce8	200	157	38	61

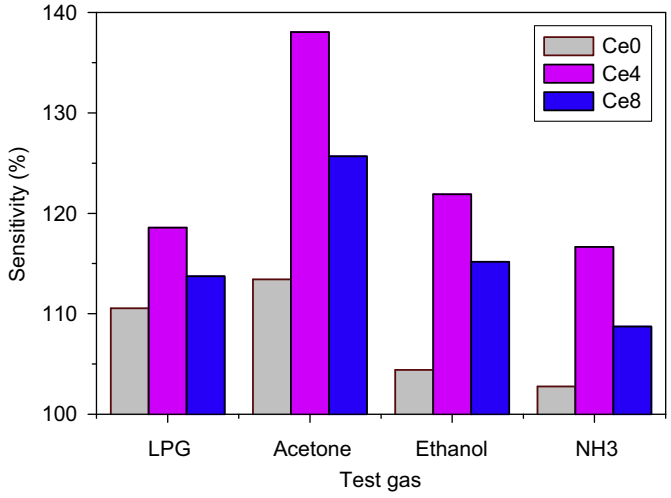

Fig. 4. Comparative gas responses of Ce0, Ce4 and Ce8 ferrite sensors towards 100 ppm concentration of test gases at 200 °C.

3.4. Acetone sensing mechanism

When exposed to a reducing gas, such as acetone vapor, the reaction between the acetone vapor and the oxygen that is adsorbed onto the surface of the undoped and doped $CoFe_2O_4$ ferrites can be expressed by[35]:

$$(CH_3)_2CO + 4O^-_{2(adsorbed)} \rightarrow 3CO_2 + 3H_2O + 8e^-_{(cb)} \quad (3)$$

The electrons are annihilated with the vacancies in the ferrite material, consequently the concentration and conductivity of the material decreases.

3.5. Response of the sensors toward 100 ppm concentration of test gases

Fig. 4 shows the observed gas response of Ce0, Ce4 and Ce8 ferrite sensors at operating temperature of 200 °C toward 100 ppm of LPG, acetone, ethanol and ammonia. The response of $CoFe_2O_4$ ferrite toward all the gases is found to be enhanced after Ce addition. Particularly for Ce4 ferrite sample the observed gas responses towards the 100 ppm of LPG, acetone, ethanol and ammonia are 119%, 138%, 122% and 117%, respectively. It is seen that the Ce4 sensor exhibits remarkable response toward lower concentrations of test gases and is found to be highly selective toward acetone at optimum temperature of 200 °C. Thus, the Ce doped $CoFe_2O_4$ material seems to be a better candidate as an acetone sensor in view of its commercial application.

4. Conclusions

Spinel-type nanocrystalline $CoFe_{2-x}Ce_xO_4$ ($x=0$, 0.04, 0.08) ferrite powders were synthesized using simple and cost effective molten-salt method. The effects of Ce doping on the structural, morphological and gas sensing properties towards LPG, acetone, ethanol and ammonnia were investigated. All the peaks in XRD patterns corresponding to the investigated systems and no unidentified peaks have been observed. Nanocrystallinity of the ferrite sample was found to play a crucial role in gas sensitivity. The gas response and selectivity strongly depends on the doping content. The Ce0 sample exhibited the selective response of 146% toward acetone at 2000 ppm at operating temperature of 350 °C. However after Ce incorporation, the sensitivity has been improved to 177% for Ce4 sample at 225 °C, while gas response decreased to 157% at 200 °C for Ce8 sample. Results showed that the 4 wt % Ce doped $CoFe_2O_4$ material exhibited good response and selectivity towards acetone vapor as compared with parent material.

Acknowledgment

Authors gratefully acknowledge CSIR and DAE-BRNS, India for the financial support.

References

[1] E. Rossinyol, J. Arbiol, F. Peiro, A. Cornet, J.R. Morante, B. Tian, T. Bo, D. Zhao, Nanostructured metal oxides synthesized by hard template method for gas sensing applications, Sensors and Actuators B 109 (2005) 57–63.
[2] C. Xiangfeng, J. Dongli, G. Yu, Z. Chenmou, Ethanol gas sensor based on $CoFe_2O_4$ nano-crystallines prepared by hydrothermal method, Sensors and Actuators B 120 (2006) 177–181.
[3] K. Mukherjee, S.B. Majumder, Reducing gas sensing behavior of nano-crystalline magnesium–zinc ferrite powders, Talanta 81 (2010) 1826–1832.
[4] N.S. Chen, X.J. Yang, E.S. Liu, J.L. Huang, Reducing gas-sensing properties of ferrite compounds MFe_2O_4 (M=Cu, Zn, Cd and Mg), Sensors and Actuators B 66 (2000) 178–180.
[5] G.A. El-Shobaky, A.M. Turky, N.Y. Mostafa, S.K. Mohamed, Effect of preparation conditions on physicochemical, surface and catalytic properties of cobalt ferrite prepared by coprecipitation, Journal of Alloys and Compounds 493 (2010) 415–422.
[6] L. Satyanarayana, K.M. Reddy, S.V. Manorama, Synthesis of nanocrystalline $Ni_{1-x}Co_xMn_xFe_{2-x}O_4$: a material for liquefied petroleum gas sensing, Sensors and Actuators B 89 (2003) 62–67.
[7] A.B. Gadkari, T.J. Shinde, P.N. Vasambekar, Effect of Sm^{3+} ion addition on gas sensing properties of $Mg_{1-x}Cd_xFe_2O_4$ system, Sensors and Actuators B 178 (2013) 34–39.
[8] Y. Chen, J.E. Snyder, C.R. Schwichtenberg, K.W. Dennis, R. W. McCallum, D.C. Jiles, Metal-bonded Co-ferrite composites for

magnetostrictive torque sensor applications, IEEE Transactions on Magnetics 35 (1999) 3652–3654.
[9] O.F. Caltun, G.S.N. Rao, K.H. Rao, B. Parvatheeswara Rao, C.G. Kim, C.O. Kim, I. Dumitru, N. Lupu, H. Chiriac, High magnetostrictive cobalt ferrite for sensor applications, Sensor Letters 5 (2007) 45–47.
[10] N. Iftimie, E. Rezlesu, P.D. Popa, N. Rezlescu, Gas sensitivity of nanocrystalline nickel ferrite, J.ournal of Optoelectronics and Advanced Materials 8 (2006) 1016–1018.
[11] Z. Tianshu, P. Hing, Z. Jiancheng, K. Lingbing, Ethanol-sensing characteristics of cadmium ferrite prepared by chemical coprecipitation, Materials Chemistry and Physics 61 (1999) 192–198.
[12] P.C Rajath Varma, R.S. Manna, D. Banerjee, M.R. Varma, K.G. Suresh, A.K. Nigam, Magnetic properties of $CoFe_2O_4$ synthesized by solid state, citrate precursor and polymerized complex methods: a comparative study, Journal of Alloys and Compounds 453 (2008) 298–303.
[13] D.S. Mathew, R.S. Juang, An overview of the structure and magnetism of spinel ferrite nanoparticles and their synthesis in microemulsions, Chemical Engineering Journal 129 (2007) 51–65.
[14] L. Lezhong, L. Zhongwen, Y. Zhong, S. Ke, J. Haining, Influence of quencher on microstructure and magnetic properties of manganese–zinc ferrites, Journal of Magnetism and Magnetic Materials 318 (2007) 39–43.
[15] H.W. Wang, S.C. Kung, Crystallization of nanosized Ni–Zn ferrite powders prepared by hydrothermal method, Journal of Magnetism and Magnetic Materials 270 (2004) 230–236.
[16] S. Chander, B.K. Srivastava, A. Krishnamurthy, Magnetic behavior of nanoparticles of $Ni_{0.5}Co_{0.5}Fe_2O_4$ preapered using two different routes, Indian Journal of Pure Applied Physics 42 (2004) 366–370.
[17] X.M. Liu, S.Y. Fu, C.J Huang, Magnetic properties of Ni ferrite nanocrystals dispersed in the silica matrix by sol–gel technique, Journal of Magnetism and Magnetic Materials 281 (2004) 234–239.
[18] B.H. Ryu, H.J. Chang, Y.M. Choi, K.J. Kong, J.O. Lee, C.G. Kim, H. K. Jung, J.H. Byun, Preparation of $Co_{1-x}Ni_xFe_2O_4$ nanoparticles by coprecipitation method, Physica Status Solidi (a) 201 (2004) 1855–1858.
[19] I.H. Gul, F. Amin, A.Z. Abbasi, M. Anis-ur-Rehman, A. Maqsood, Physical and magnetic characterization of co-precipitated nanosize Co–Ni ferrites, Scripta Materialia 56 (2007) 497–500.
[20] M.S. Khandekar, R.C. Kambale, S.S. Latthe, J.Y. Patil, P.A. Shaikh, N. Hur, S.S. Suryavanshi, Role of fuels on intrinsic and extrinsic properties of $CoFe_2O_4$ synthesized by combustion method, Materials Letters 65 (2011) 2972–2974.
[21] S.L. Darshane, R.G. Deshmukh, S.S. Suryavanshi, I.S. Mulla, Gas-sensing properties of zinc ferrite nanoparticles synthesized by the molten-salt route, Journal of the American Ceramic Society 91 (2008) 2724–2726.
[22] N.L. Tarwal, P.S. Shinde, Y.W. Oh, Romana Cerc Korošec, P.S. Patil, Nickel-induced microwheel-like surface morphological evolution of ZnO thin films by spray pyrolysis, Applied Physics A 109 (2012) 591–599.
[23] J.Y. Patil, A.V Rajgure, L.K Bagal, R.C Pawar, I.S Mulla, S. S Suryavanshi, Structural, morphological, and gas response properties of citrate gel synthesized nanocrystalline ZnO and $Zn_{0.9}Cd_{0.1}O$ materials, Ceramics International 39 (2013) 4383–4390.
[24] N.L. Tarwal, P.S. Patil, Enhanced photoelectrochemical performance of Ag–ZnO thin films synthesized by spray pyrolysis technique, Electrochimica Acta 56 (2011) 6510–6516.
[25] X.P. Peng, J.Z. Xu, H. Zang, B.Y. Wang, Z.G. Wang, Structural and PL properties of Cu-doped ZnO films, Journal of Luminesence 128 (2008) 297–300.
[26] N.L. Tarwal, R.S. Devan, Y.R. Ma, R.S. Patil, M.M. Karanjkar, P. S. Patil, Spray deposited localized surface plasmonic Au–ZnO nanocomposites for solar cell application, Electrochimica Acta 72 (2012) 32–39.
[27] A.B. Bodade, A.B. Bodade, H.G. Wankhade, G.N. Chaudhari, D. C. Kothari, Conduction mechanism and gas sensing properties of $CoFe_2O_4$ nanocomposite thick films for H_2S gas, Talanta 89 (2012) 183–188.
[28] L.K. Bagal, J.Y. Patil, I.S. Mulla, S.S. Suryavanshi, Influence of Pd-loading on gas sensing characteristics of SnO_2 thick films, Ceramics International 38 (2012) 4835–4844.
[29] K.V. Gurav, P.R. Deshmukh, C.D. Lokhande, LPG sensing properties of Pd-sensitized vertically aligned ZnO nanorods, Sensors and Actuators B 151 (2011) 365–369.
[30] M.S. Khandekar, N.L. Tarwal, J.Y. Patil, F.I. Shaikh, I.S. Mulla, S. S Suryavanshi, Liquefied petroleum gas sensing performance of cerium doped copper ferrite, Ceramics International 39 (2013) 5901–5907.
[31] S.L. Darshane, S.S. Suryavanshi, I.S. Mulla, Nanostructured nickel ferrite: a liquid petroleum gas sensor, Ceramics International 35 (2009) 1793–1797.
[32] N. Rezlescu, E. Rezlescu, C. Pasnicu, M.L. Craus, Effects of the rare-earth ions on some properties of a nickel-zinc ferrite, Journal of Physics D: Condensed Matter 6 (1994) 5707–5716.
[33] C.H. Shin, D.S. Lee, S.I. Hwang, M.B. Lee, J.S. Huh, D.D. Lee, Gas sensing characteristics of SnO_2 thin film fabricated by thermal oxidation of a Sn/Pt double layer, Sensors and Actuators B 81 (2002) 176–181.
[34] X. Niu, W. Du, Preparation and gas sensing properties of ZnM_2O_4 (M=Fe, Co, Cr), Sensors and Actuators B 99 (2004) 405–409.
[35] N.L. Tarwal, A.V. Rajgure, A.I. Inamdar, R.S. Devan, I.Y. Kim, S. S. Suryavanshi, Y.R. Ma, J.H. Kim, P.S. Patil, Growth of multifunctional ZnO thin films by spray pyrolysis technique, Sensors Actuators A: Physics 199 (2013) 67–73.